Structural and Optical Isomers of Nonamethoxy Cyclotriveratrylene: Separation and Physical Characterization

Zeev Luz,*,† Raphy Poupko,† Ellen J. Wachtel,† Hailin Zheng,† Noga Friedman,† Xiaolin Cao,‡ Teresa B. Freedman,‡ Laurence A. Nafie,‡ and Herbert Zimmermann§

Weizmann Institute of Science, Rehovot 76100, Israel, Department of Chemistry, Syracuse University, Syracuse, New York 13244, and Max-Planck-Institute for Medical Research, Jahnstrasse 29, 69120 Heidelberg, Germany

Received: May 1, 2007; In Final Form: July 5, 2007

The paper concerns the structural and optical isomers of nonamethoxy-tribenzocyclononene (compound **1**). In the first part of the paper it is shown that **1** exists in two structural isomers: a rigid crown (c-**1**) with C_3 symmetry and a flexible saddle (s-**1**) with C_1 symmetry. The latter, not previously known, can be prepared from the as-synthesized c-**1** by quenching a hot solution (or the melt) followed by HPLC separation. The crown/saddle equilibrium, isomerization kinetics, and associated thermodynamic parameters in various organic solvents are reported. Carbon-13 MAS NMR, X-ray diffraction, and differential scanning calorimetry (DSC) of polycrystalline c-**1** and s-**1** racemates are also reported. The different melting points of the isomers and their rapid isomerization in the melt result in unconventional DSC thermograms involving multiple endothermic and exothermic transitions. The second part of the paper concerns the chiral properties of **1**. Both the saddle and crown isomers are structurally chiral, but due to the fast pseudorotation of s-**1** in solution, it cannot be separated into its enantiomers. Those of c-**1** were separated by HPLC using a chiral column. Their X-ray structure and melting points differ considerably from those of the racemate. This and their fast racemization in the melt lead to complex DSC thermograms with multiple transitions. Solutions of the neat enantiomers exhibit a relatively small specific optical rotation. In the UV they show circular dichroism for the B_{1u} and B_{2u} transitions, with the latter exhibiting a clear couplet structure. Infrared and vibrational circular dichroism spectra of the enantiomers in solution are reported. Comparison of these spectra with quantum mechanical simulations provides unambiguous identification of the enantiomers.

Introduction

The derivatives of the tribenzocyclononene (TBCN) core are often referred to as cyclotriveratrylenes after their parent compound (hexamethoxy-TBCN).[1] Interest in these compounds[2−5] stems from their tendency to form molecular complexes in solution as well as inclusion compounds in the solid state and from their mesogenic properties when substituted with sufficiently long side chains.[6,7] They also serve as starting materials for the powerful crypthophane caging agents.[8,9] Cyclotriveratrylenes can exist in two structural isomers: crown and saddle (see Figure 1). The crown form is structurally rigid and usually the thermodynamically more stable isomer (at room temperature and below), while the saddle isomer is highly flexible, undergoing (in solution and the melt) extremely fast pseudorotation. The lower stability of the saddle form (or rather the twisted saddle) is attributed to the repulsive interaction between the inward pointing methylene hydrogen and the oppositely positioned phenyl ring. According to theoretical calculations it amounts to a destabilization of about 15−20 kJ/mol relative to the corresponding crown isomer.[2−4] It can be stabilized, relative to the corresponding crown, by substituting bulky groups ortho to the ring methylene or chemically modifying the latter. For that reason it has been assumed that peripherally substituted CTV's can only exist in the crown form. In derivatives exhibiting both isomers, the crown−saddle isomerization is usually very slow at room temperature. Consequently, they can be separated (for example, by chromatography) and kept in their neat form for long periods (in solution for weeks and months and much longer in the solid state or under cooling).[10]

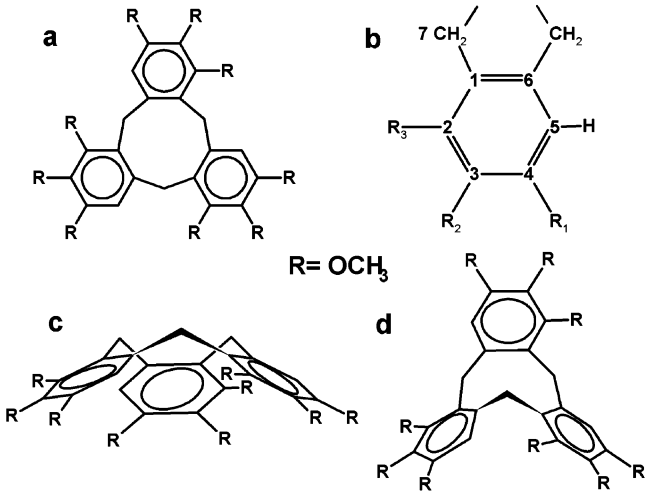

Figure 1. (a) Molecular formula of nonamethoxy TBCN. (b) Numbering system used in the present paper. (c) Molecular structure of the crown isomer. (d) Molecular structure of the saddle isomer.

In a recent publication[11] we presented a detailed study of the parent CTV compound in the neat solid state and solutions. In contrast to the generally accepted belief, it was found that this peripherally substituted derivative can, in fact, be prepared in

† Wiezmann Institute of Science.
‡ Syracuse University.
§ Max-Planck-Institute for Medical Research.

10.1021/jp073329g CCC: $37.00
Published on Web 10/03/2007

the saddle form and that this isomer is sufficiently stable to allow detailed structural and kinetic investigations in both the solid state and solution. In the present paper we extend this study to the nonamethoxy derivative of TBCN with C_3 symmetry (Figure 1). It was reported earlier[4] that, like the parent CTV, this derivative only exists in the crown isomer, the ortho methoxy group being too small to efficiently destabilize it. In fact, the saddle isomer of this derivative can be prepared and is sufficiently stable to allow physical characterization. The failure to detect the saddle isomers of these compounds (CTV and its nonamethoxy derivative) in the past stems from the procedure used in their synthesis, i.e., acidic condensation of the correspondingly substituted benzyl alcohols at moderate temperatures. Under these conditions the crown form is preferentially formed and any coexisting small amounts of saddle in the reaction mixture are washed away during the purification process. Once the crown isomer is recovered the saddle isomer will usually not form even after being kept for a long time at moderate temperatures because of the very high activation barrier of the crown−saddle isomerization. The saddle isomer can, however, be generated by heating the melt or a solution of the crown isomer to sufficiently high temperatures where the saddle isomer is favored thermodynamically (because of its higher entropy) and where the isomerization rate is fast.[10,11] The hot liquid is then quenched, freezing-in the high-temperature saddle/crown equilibrium ratio, which depending on the solvent and temperatures may be as high as unity or even higher. The saddle and crown isomers can then be quantitatively separated by chromatography at room temperature where isomerization is negligible. We used this procedure to prepare macroscopic amounts of both the crown and saddle isomers of nonamethoxy TBCN and performed detailed structural and kinetic measurements using X-ray, DSC, and NMR techniques. In the first part of this paper we describe the results of these measurements in both the solid state and solution.

The isomers of nonamethoxy TBCN (C_3 symmetry) lack symmetry planes and thus belong to the family of TBCN derivatives which are structurally chiral.[12,13] Such derivatives can therefore, in principle, be separated into their corresponding enantiomers. In practice, due to their fast pseudorotation (in solution) the saddle isomers rapidly racemize, precluding such separation. On the other hand, racemization of the crown isomers of chiral CTV's (which most likely proceeds via their saddle forms)[11,14] is usually very slow at room temperature, allowing their enantioseparation or the selective chemical preparation of a particular enantiomer. This latter approach was extensively used by Collet, Gottarelli, and co-workers[15−21] to synthesize neat enantiomers of (or enantiomerically enriched) hexa- (and tri-) peripherally substituted CTV's with C_3 symmetry ($R_3 = H$, $R_1 \neq R_2$). Their absolute configuration was derived from that of the diastereogenic starting compounds (whose structure was determined by X-ray measurements).[22] The consistency of the results was confirmed by analysis of their UV circular dichroism (UVCD) spectra, and their enantiomeric excess was determined by analytical HPLC using chiral columns.[23]

In the present investigation of the chiral crown isomer of nonamethoxy TBCN, rather than performing an elaborate asymmetric synthesis, we separated its racemate by semipreparative chiral HPLC. We studied the physical and optical properties of these enantiomers in the solid state and solutions and compared them with those of the racemate. Using infrared vibrational circular dichroism (VCD)[24,25] we were, in fact, able to determine their absolute configuration. By the UPAC rules these enantiomers are labeled *M* and *P*, as shown in Figure 2.[22]

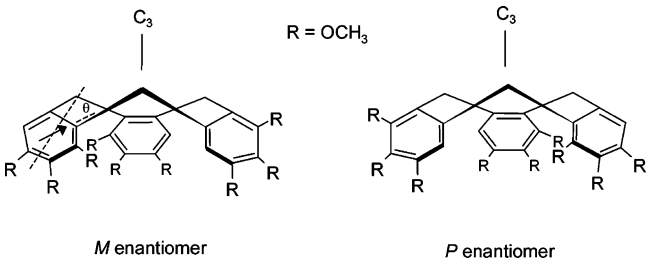

Figure 2. Absolute configurations of the *M* and *P* enantiomers of c-**1**. θ is the angle between the short axis of the benzene ring and the B_{2u} transition moment (arrow). It is positive for a clockwise rotation.

As it turned out the enantiomer to elute first from the HPLC column has the *P* configuration, while the second corresponds to the *M* configuration. The details of the measurements on the optical crown isomers are described in the second part of the paper.

In the following we refer to the nonamethoxy TBCN derivative as **1** and label its crown and saddle isomers as c-**1** and s-**1**, respectively. The enantiomers of the optically active crown isomers are labeled *A* and *B*, according to their elution order (*A* first, *B* second) from the HPLC column.

Experimental Section

Synthesis and Enantioseparation of the Crown Form. Compound **1** was synthesized by condensation of 2,3,4-trimethoxybenzyl alcohol in 10% sulfuric acid under reflux.[10,26] The final product was crystallized several times from ethanol. The compound so obtained was entirely in the crown racemic form, c-**1**, with at most traces of the saddle isomer (s-**1**). This material was used to prepare the pure optical isomers of the crown form as well as the neat saddle isomer as also described in ref 13.

Separation of the crown isomer into its enantiomers was accomplished using a semipreparative HPLC column (25 cm L × 2 cm I.D.) equipped with a guard column (2.0 cm L × 1.0 cm I.D.), both of which were packed with 5 μm silica particles coated with a polysaccharide as the chiral stationary phase (CHIRALCELOD-H, Chiral Technologies Europe). A 1/1 MeOH/EtOH mixture served as the mobile phase with a flow rate of 10 mL/min. The detection wavelength was 254 nm. Typically, a solution of about 450 mg of **1** in 50 mL of acetonitrile/MeOH (1/1) was used as the injecting solution. An example of a chromatogram for a 1 mL injection is shown in the bottom trace of Figure 3. The weak peak at about 10 min was identified by ^{1}H NMR as due to the saddle isomer. The succeeding two intense peaks at about 12 and 22 min are due to the crown enantiomers of **1**. They are labeled as *A* and *B*, according to the order at which they emerge from the column. Satisfactory baseline resolution could be obtained with injections of up to 5 mL. The latter figure was used in practice in the separation procedure. The neat enantiomers were obtained in dry solid form by evaporating the mobile phase under reduced pressure at room temperature, redissolved in ether, and dried again. Injection of solutions of the separated enantiomers into the same semipreparative columns showed them to be optically pure. The chiral purity was also confirmed by ^{13}C NMR spectra in chiral lyotropic liquid crystalline solutions based on poly-γ-benzyl-L-glutamate.[13] In such solutions the spectra of the two enantiomers are well resolved and those of the separated enantiomers did not show enantiocontamination. Typical yields: 85 mg of enantiomer *A* and 120 mg of enantiomer *B*. The lower yield of *A* is due to the partial overlapping with the saddle peak. Solutions and solid samples of the enantiomers

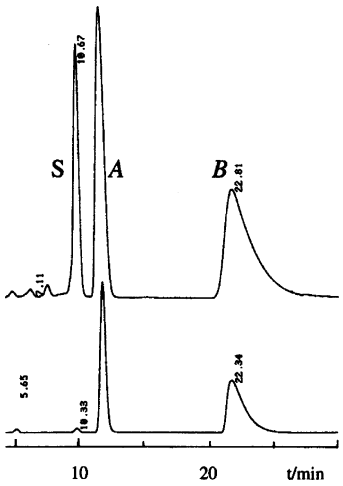

Figure 3. HPLC chromatograms of compound **1**. (Bottom) Obtained after purification of the as-synthesized crown isomer. (Top) Obtained from a sample crystallized from a quenched DMSO solution (170 °C). The latter contains about 25% saddle. The peaks S, *A*, and *B* (at about 10, 12, and 22 min) correspond, respectively, to the saddle isomer and the crown *A* and crown *B* enantiomers. Some weak peaks preceding the saddle signal are due to impurities from the column.

were kept in the cold when not in use to minimize chances of racemization.

Preparation and Separation of the Saddle Form. For the preparation of the neat saddle form, s-**1**, we made use of the fact that the saddle/crown equilibrium ratio, in solution, increases steeply with increasing temperature and that the isomerization is rapid at high temperatures and very slow at room temperature and below. Accordingly,[11,13] we dissolved the as-synthesized crown form, c-**1**, in a high boiling point solvent [dimethylsulfoxide (DMSO) or tetraglyme (tetraethylene glycol dimethyl ether)] and heated the solution to the highest possible temperature (170 and 265 °C, respectively). The hot solution was then quenched by splashing it into a crushed-ice/water/NaCl bath. After the mixture thawed it was filtered, washed with water, and dried by lengthy pumping. Proton NMR of the product showed signals from both the saddle and crown isomers. The saddle/crown ratio was about 1/3 and 1/1 for the material recovered from DMSO and tetraglyme solutions, respectively. Thin layer chromatography (silica, ether/CH_2Cl_2) gave two poorly resolved spots due to the two isomers.

Separation of these saddle and crown isomers from this mixture by regular liquid chromatography as used for the CTV[11] proved quite inefficient, producing just a few milligrams of the saddle isomer even when meters long columns were used. Fortunately, as it turned out, the chiral HPLC column used to separate the crown enantiomers was also found to be useful for separation of the saddle isomer. To demonstrate the resolution of the method we show in the top trace of Figure 3 HPLC chromatograms of the material obtained by quenching a hot DMSO solution. The s-**1** so obtained was purified as described above for the crown enantiomers.

Physical Measurements. Differential scanning calorimetry (DSC) measurements were performed on a Mettler DSC30 instrument.

X-ray diffraction profiles of powder samples were measured on a D-Max/B diffractometer (Rigaku, Japan) affixed to a RU-200 rotating anode X-ray generator (Rigaku) operating with a copper anode at 7 kW ($\lambda = 0.154$ nm).

Proton and ^{13}C high-resolution NMR were recorded on a DRX-400 Bruker spectrometer operating at 400.13 and 100.62 MHz, respectively. Carbon-13 magic angle spinning (MAS) NMR spectra of solid samples were recorded on a DSX-300 Bruker spectrometer using 4 mm spinners.

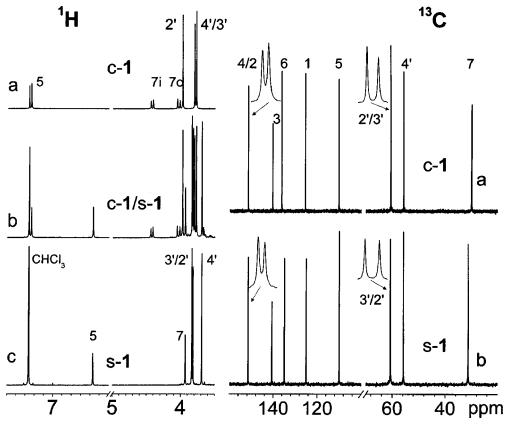

Figure 4. Proton (left) and ^{13}C (right) NMR spectra of the crown and saddle racemates of **1** in chloroform solutions. On the left side, a and c correspond to the crown and saddle isomers, respectively, and b to a sample obtained by quenching a solution of **1** in tetraglyme from 265 °C. The ^{13}C spectra on the right are of the crown (a) and saddle (b) isomers. The labeling of the peaks is according to the numbering system in Figure 1b. Primed numbers indicate methoxy groups linked to corresponding aromatic carbons.

UV spectra (in the wavelength range 210−330 nm) were recorded on a single-beam AGILENT spectrophotometer (model 8453) with diode array detection. The UVCD spectra were recorded on an Aviv circular dichroism spectrometer, model 202. For both types of measurements 10.0 and 1.0 mm path length quartz cells were used with ethanol as the solvent. Optical rotation was measured in chloroform solutions with a Perkin-Elmer Polarimeter, model 341, using a 10.0 cm path length quartz cell (total volume of solution, 1 mL) and 20 s integration times.

IR and VCD spectra were recorded with a modified Chiral*IR* FT-VCD spectrometer (BioTools, Inc. Wauconda, IL). The samples were placed in 0.10 mm path length cells with BaF_2 windows. The measurements covered the range 1800−1000 cm^{-1} with the spectrometer optimized at 1400 cm^{-1}. They were made with 4 cm^{-1} resolution and 5 h collection time. All the spectroscopic calculations were done on the *P* (*A*) enantiomer (Figure 2). Its conformation was constructed with HyperChem software (Hypercube, Inc., Gainsville, FL). Calculation of its optimized geometry as well as its vibrational frequencies and IR and VCD intensities (requiring 8.5 days CPU time) were carried out at the DFT level (6-31G(d) basis set/B3LYP functional) with Gaussian 03W on a Pentium IVPC. Calculated frequencies were uniformly scaled by 0.97, and the calculated intensities were converted to Lorentzian bands with 6 cm^{-1} half width for comparison with the experiment.

Results and Discussion

A. Crown and Saddle Racemates. *1. NMR Spectra and the Saddle−Crown Isomerization in Solution.* The solution ^1H and ^{13}C NMR spectra of the isomers of **1** were extensively studied by Lafont et al.[13] The ^1H spectrum is especially suitable for identifying the saddle and crown isomers (see Figure 4, left). In particular, the ring methylene protons exhibit an AB quartet (centered at 4.23 ppm, $J = 13.6$ Hz) for the crown and a singlet (at 3.93 ppm) for the saddle. This singlet reflects the fast pseudorotation of the saddle isomer, which averages the chemical shifts of all the methylene hydrogens. Also, there is a significant chemical shift difference for the aromatic hydrogens in the two isomers (7.24 and 6.57 ppm for the crown and saddle, respectively). We used such ^1H spectra to determine the saddle/

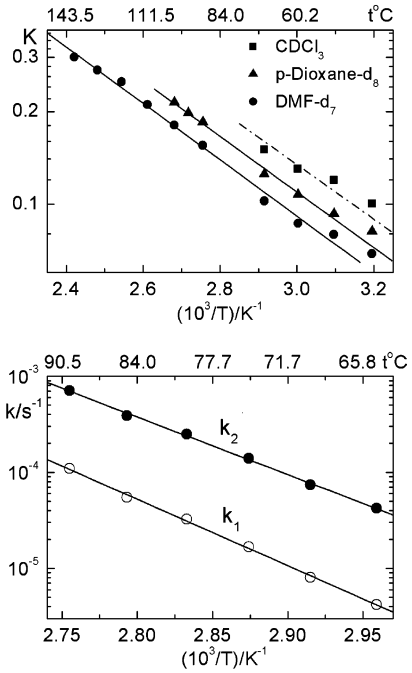

Figure 5. Temperature dependence of the thermodynamic parameters for the saddle/crown equilibrium and interconversion rate of **1**. (top) K = [saddle]/[crown] for different solvents as indicated. (bottom) Rate constants for the crown to saddle (k_1) and saddle to crown (k_2) in DMF-d_7.

crown ratio in quenched samples prepared as described in the Experimental Section. An example is shown in the middle trace of Figure 4 (left). This spectrum applies to a sample obtained by quenching a solution of **1** in tetraglyme from 265 °C. It is readily seen that it corresponds to a saddle/crown ratio of about 1/1. On the other hand, the carbon-13 spectra of the two isomers are very similar (Figure 4, right). This too reflects the fast pseudorotation of the saddle, which renders the aromatic rings equivalent, as they are in the crown. The labeling of the signals in the spectra is according to the numbering system in Figure 1b and was adopted from ref 13. This assignment will be useful in identifying the peaks in the ^{13}C MAS spectra of the solid samples.

We used the solution ^{1}H NMR spectrum to determine the saddle/crown equilibrium ratio, K, and interconversion rates, k_1 and k_2, as a function of the temperature in a number of solvents

$$\text{crown} \underset{k_2}{\overset{k_1}{\rightleftharpoons}} \text{saddle} \qquad K = k_1/k_2 = [\text{saddle}]/[\text{crown}]$$

For determination of the equilibrium constant solutions containing about 2 mg of **1** in 1 mL of the desired solvent were placed in a thermostated bath in the range 40−70 °C. ^{1}H NMR spectra were recorded at room temperature at regular time intervals until the relative intensity of the signals due to the saddle and crown isomers remained constant. At 90 °C and higher the measurements were performed in a heated NMR probe. The equilibrium constant was then determined from the relative intensity of the corresponding aromatic peaks. Measurements were performed in deuterated DMF, chloroform, and *p*-dioxane. The results are plotted versus the inverse absolute temperature in the top of Figure 5. Analysis of these results in terms of the equilibrium equation

$$K = K_\infty \exp(-\Delta H/RT) = \exp[(T\Delta S - \Delta H)/RT]$$

yields the thermodynamic parameters summarized in Table 1a, where they are compared with those for CTV.

The saddle−crown isomerization kinetics were studied in a similar way by following the changes with time of the NMR signals at different temperatures. Measurements were performed in DMF between 65 and 90 °C, starting with a solution of the neat saddle. Analysis was performed as described in refs10 and 11, and the results for k_1 and k_2 are shown in the bottom of Figure 5. The parameters derived from these measurements, in terms of Eyring's equation

$$k = A \exp(-E_a/RT) = (\kappa kT/h)\exp[(T\Delta S^* - \Delta H^*)/RT]$$

are summarized in Table 1b. Prominent features of these results are the high ΔS value of the equilibrium constant, which reflects the high flexibility of the saddle isomer as compared to the rigid crown form, and the very high activation energy for their interconversion. The latter parameter is even higher than that for CTV, probably due to extra hindrance of the ortho methoxy group in the transition state.

2. DSC and the Saddle−Crown Isomerization in the Solid State. In the solid state at room temperature the crown and saddle racemates are stable and may be kept for long periods without undergoing isomerization. However, at higher temperatures in the solid−melt interface the systems exhibit peculiar phase diagrams involving saddle−crown interconversion. This is demonstrated in the series of DSC thermograms on the left-hand side of Figure 6. The transition temperatures and enthalpies derived from these thermograms are summarized in the first four entries of Table 2.

Trace a in this figure corresponds to the first heating of a neat crown sample with a single melting transition at 205.4 °C. A considerably more complicated diagram is obtained for the saddle isomer (trace d). As a function of increasing temperature it exhibits first an endothermic melting transition at 117.8 °C, followed by an exothermic peak at 130.3 °C, and finally a second melting at 202.0 °C. This thermogram is similar to that observed for the mesogenic and nonmesogenic saddle homologues of the nonaalkanoyloxy TBCN series.[10] In the present case we identify the first endothermic transition with the melting transition of the saddle isomer. In the melt, fast saddle−crown isomerization sets in and an equilibrium is established with [saddle]/[crown] ≈ 1/3 (see below). The melt is thus predominantly crown, which in this temperature range prefers the solid state. Hence, it solidifies exothermally (peak at 130.3 °C). As solidification progresses the equilibrium in the melt drives more and more of the saddle to the crown form until the entire sample is crystallized in the racemic crown form. This sequence of events is confirmed by observation with a polarizing optical microscope (equipped with a hot stage). At 117 °C formation of a liquid is observed, which rapidly solidified upon further heating. High-resolution ^{1}H NMR of a solution of this solid confirmed it to be entirely of the crown isomer. This is also borne out by the second melting transition in the DSC thermogram, which corresponds to that of the crown, as in trace a.

When the hot melt obtained by heating the crown, as in a, or the saddle, as in d, is slowly (1−2 K/min) cooled through the 205−200 °C region down to room temperature and the resulting solid re-examined by DSC, a thermogram similar to that of a is obtained. This identifies the solid as neat crown, as also confirmed by its ^{1}H NMR spectrum. If, however, the melt is rapidly (>10 K/min) cooled through the melting region it is found (by ^{1}H NMR) that the resulting solid consists of a saddle/crown ≈ 1/3 mixture. When this solid is reheated, a thermogram as shown in trace b is obtained. It exhibits a broad exothermic peak in the range 110−135 °C followed by a melting transition

TABLE 1: Thermodynamic Parameters for the Saddle/Crown Equilibrium and Saddle/Crown Interconversion for 1, and Comparison with Similar Data for CTV[11]

Arrhenius parameters[a]					
compound	solvent	K_∞	ΔH (kJ/mol)	ΔS (J/mol.K)	$K(300)$
1	$CDCl_3$[b]	(64.5)	(17.1)	(34.6)	(0.07)
1	*p*-dioxane-d_8	54.6 ± 12.2	17.2 ± 0.7	33.3 ± 1.8	0.055
1	DMF-d_7	51.8 ± 9.5	17.6 ± 0.6	32.8 ± 1.5	0.045
CTV	$CDCl_3$	5.3 ± 1.0	10.0 ± 0.5	13.8 ± 1.6	0.097
CTV	DMF-d_7	59.7 ± 24	22.3 ± 1.2	34.0 ± 3.2	0.008

Eyring parameters[c]					
compound	solvent	log A (s^{-1})	E_a (kJ/mol)	ΔH^* (kJ/mol)	ΔS^* (J/mol·K)
1	DMF-d_7	15.1 ± 0.6	132.2 ± 3.8	129.7 ± 3.8	35.3 ± 10.8
CTV	$CDCl_3$	11.0 ± 0.8	97.4 ± 4.8	94.9 ± 4.8	-43.5 ± 15.0

[a] Arrhenius parameters for the equilibrium constant K = [saddle]/[crown]. $K = \exp(-\Delta G/RT) = K_\infty \exp(-\Delta H/RT)$, $K_\infty = \exp(\Delta S/R)$. [b] Line drawn parallel to those in the other solvents and is not a best-fit result. [c] Eyring parameters for the rate constant, k_1 (crown to saddle).

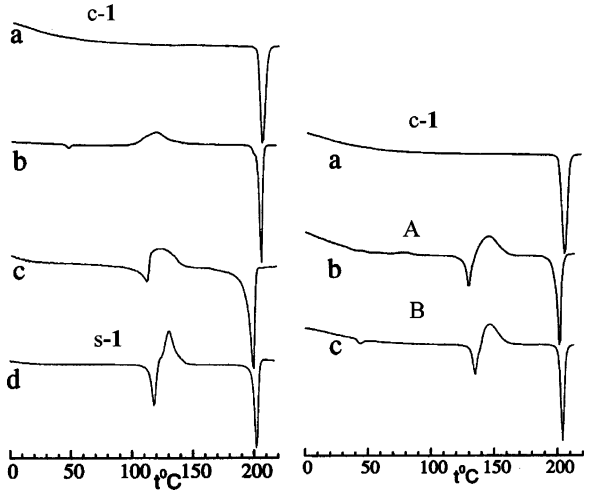

Figure 6. DSC thermograms of different samples of **1** (heating rate, 10 K/min). (Left) Results for racemic crown and saddle. (a) First heating of the crown racemate. (b) Second heating of sample (a) after rapidly cooling the melt from just above the melting point (the sample contained about 25% saddle). (c) First heating of a sample obtained by quenching a tetraglyme solution from 265 °C (the sample contained about 50% saddle). (d) First heating of a neat saddle sample. (Right) (a) Same as a on the left. (b and c) First heating of neat enantiomers *A* and *B*, respectively.

at 204.4 °C. Proton NMR measurements on samples removed above this exothermic transition (but below the melting) showed it to be entirely in the crown form. Clearly rapid cooling (or quenching) freezes in the equilibrium saddle−crown ratio of the melt, resulting in a solid mixture of the two isomers. The exothermic peak (around 120 °C) thus reflects the conversion of the extra saddle isomer to the crown form. Since no liquid was observed in this temperature range under a polarizing microscope the transformation is evidently a solid-state reaction. The particular thermogram of trace b was recorded 3 days after quenching the melt. When a thermogram is recorded shortly after quenching a similar trace is obtained but with a much broader exothermic peak. Apparently, the quenching produces finely dispersed saddle particles, resulting in a broad transformation region. Under aging the particles becomes coarser and the distribution narrower. This trace also shows an endothermic peak at 46.7 °C, most likely due to a solid−solid transition.

Finally, we turn to thermogram c, obtained from a sample produced by quenching a solution of **1** in tetraglyme at 265 °C. The [saddle]/[crown] ratio in this sample (as determined by ^{1}H NMR) is ∼1/1. The thermogram can readily be explained in terms of the sequence (endothermic) melting of the saddle part (111.1 °C), isomerization and (exothermic) crystallization of the melt (122.6 °C), and finally (endothermic) melting of the (now entirely crown) sample (198.3 °C).

These results show that by proper heating and cooling cycles one can obtain a range of isomeric mixtures of **1** from pure crown to samples highly enriched (but not entirely neat) saddle.

3. Carbon-13 MAS NMR of the Crown and Saddle Racemates. Some information on the molecular and crystal structure of the crown and saddle racemates of **1** in the solid state could be derived from their ^{13}C MAS spectra, examples of which are shown in traces a and b of Figure 7. The assignment of the spectral bands is based on the solution spectra described above (Figure 4) and similar spectra recorded for the ^{2}H and ^{13}C isotopomers.[13] Despite some degree of overlap, the spectra are well resolved and the separate peaks are rather sharp, indicating that the samples are (poly)crystalline (rather than amorphous).

Referring first to the saddle isomer (trace b) we note that its molecular symmetry is C_1 and all carbon atoms in the molecule are nonequivalent. For a single molecule per asymmetric unit we would therefore expect 3 CH_2, 9 OCH_3, and 18 (three for each type of the benzene carbons) aromatic peaks. Except for some peak overlap, such a structure is in fact observed for the saddle spectrum. Note, in particular, the well-resolved multiplets due to the methylene (3 peaks), methoxy (9), and aromatic carbons 5 (1 + 2) and 1 (3). Since the material is racemic we may safely conclude that the asymmetric unit contains a single molecule (enantiomer), while the unit cell contains a pair of enantiomers related to each other by a symmetry element of the second kind. From the spectrum structure it also follows that the fast pseudorotation, prevailing in the liquid, is completely frozen out in the solid with the molecules locked in their crystallographic sites.

The symmetry of an ideal crown molecule is C_3, and accordingly, we could expect a simpler ^{13}C MAS spectrum than that for the saddle. In fact, the spectra of both isomers are quite similar (traces a and b of Figure 7). The main difference is in the methylene signal, which consists of a well-separated triplet in the saddle spectrum and a weakly structured singlet in the crown. However, all other signals exhibit multiplet structure, which indicates inequivalence of the benzene rings. Close examination of the aromatic bands shows that the multiplets consist of at most three peaks for each type of carbon. It is most clearly seen for the aromatic carbons 1 and 5. We therefore conclude that the crown molecules are distorted in the crystal from C_3 symmetry and that like for the saddle racemate there is a single molecule per asymmetric unit and a pair of symmetry related enantiomers per unit cell. This conclusion is borne out

TABLE 2: Phase Diagrams of Various Solid Samples of 1 Obtained by DSC Measurements[a]

sample no. (trace)[b]	sample (heating cycle)	endothermic transition (°C), ΔH (kJ/mol)[c]	exothermic transition (°C), ΔH (kJ/mol)[d]	melting transition (°C), ΔH (kJ/mol)[e]
1, L & R (a)	neat crown (first heating)			205.4 (66.9)
2, L (b)	neat crown (second heating)[f]		118.4 (−44.0)	204.4 (63.8)
3, L (c)	quenched (first heating)	111.1 (8.8)	122.6 (−29.4)	198.3 (57.4)
4, L (d)	neat saddle (first heating)	117.8 (41.4)	130.3 (−45.5)	202.2 (66.7)
5, R (b)	enantiomer *A* (first heating)	130.4 (22.7)	146.7 (−46.4)	202.0 (65.6)
6, R (c)	enantiomer *B* (first heating)	135.1 (21.4)	147.4 (−49.2)	203.9 (62.4)

[a] All thermograms correspond to heating at a rate of 10 K/min. [b] Entries 1−4 refer to the DSC thermograms on the left (L) side of Figure 6; entries 5 and 6 refer to the two bottom traces on the right (R) side of Figure 6. [c] This endothermic transition corresponds to the melting of the saddle in samples 3 and 4 and to the melting of the crown enantiomers in samples 5 and 6. [d] This exothermic transition is usually broad and corresponds in sample 2 to the saddle → crown conversion in the solid state, to the saddle → crown conversion in the melt and crystallization of the latter in samples 3 and 4, and to the racemization followed by crystallization of the neat crown enantiomers in samples 5 and 6. [e] In all cases this transition corresponds to the melting of the crown racemate. [f] Second heating after rapid cooling of the melt of 1. This sample was measured 3 days after the first run. Its DSC also showed a weak endothermic peak ($\Delta H = 2.4$ kJ/mol) at 46.7 °C, apparently due to a solid−solid transition.

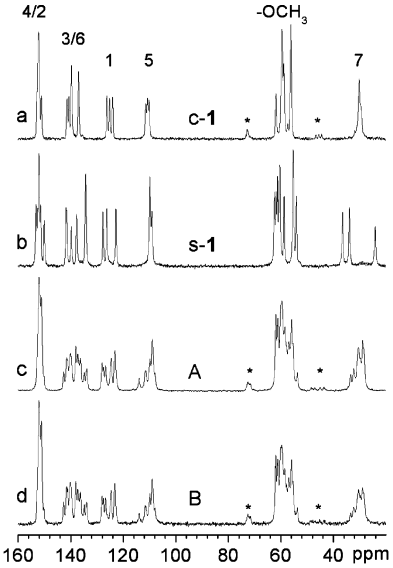

Figure 7. Carbon-13 MAS NMR spectra (100.62 MHz) of solid samples of **1**. The spectra were recorded at room temperature with a spinning rate of 6.0 kHz for traces a, c, and d and 9.3 kHz for trace b. (a and b) Racemic crown and saddle, respectively. (c and d) Neat enantiomers *A* and *B* of the crown form, respectively. Labeling of the carbon atoms is according to the notation of Figure 1b. Asterisks indicate spinning side bands.

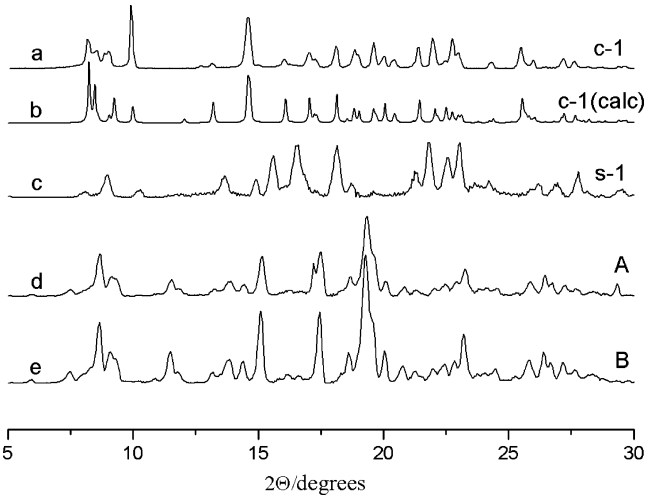

Figure 8. Room-temperature powder X-ray diffraction patterns ($\lambda = 0.154$ nm) of compound **1**: (a) racemic crown, (b) pattern calculated from X-ray structure of a single-crystal crown racemate, (c) racemic saddle, (d and e) neat enantiomers *A* and *B*, respectively.

by the X-ray measurements on a single crystal of the crown racemate, as described in the next section.

4. X-ray Measurements of the Crown and Saddle Racemates. A full X-ray structure is only available for the crown racemate form of **1**. In this form large and good quality crystals can be obtained by crystallization from solution without fear of transformation to another form. Crystallization of the saddle isomer or the neat crown enantiomers might, unless special low-temperature procedures are used, result in isomerization or racemization during crystal growth. Therefore, no full single-crystal X-ray structures are available for the latter. The X-ray structure of the crown racemate was determined by Salmon et al.[27] in 1995 and independently by Krieger[28,29] in 1998 on crystals obtained, respectively, from acetone/hexane and boiling ethanol. In both cases the structure was found to be triclinic, belonging to the $P\bar{1}$ space group (No. 2 in the International Tables of X-ray Crystallography) with unit cell dimensions $a = 11.022$ Å, $b = 12.039$ Å, $c = 12.984$ Å, $\alpha = 113.83°$, $\beta = 108.17°$, $\gamma = 100.70°$. There are two molecules per unit cell related by inversion symmetry; hence, they correspond to an enantiomeric pair. Analysis of the data also indicates that the molecules are strongly distorted from C_3 symmetry. These results are in full agreement with those of the ^{13}C MAS NMR described in the previous section.

To check whether the structure of the single crystals obtained by crystallization from boiling ethanol (used for X-ray structure determination) is the same as that of the crystallites in the powder obtained by evaporation of the solvent at room temperature (and used for the NMR MAS measurements) we compared the experimental powder diffraction of the latter with the powder diffraction pattern generated from the X-ray single-crystal data[28,29] using the computer program Mercury 1.2.1. As seen in traces a and b of Figure 8, the two diffractograms are quite similar, in particular with respect to the peak positions. The similarity is not as perfect with respect to the peak intensities. We may attribute this to nonrandom crystallite distribution in the powder and conclude that the crystal structures of both systems are, in fact, the same.

As indicated, we were unable to grow single crystals of the racemic saddle isomer. The powder diffraction pattern of this compound is shown in trace c of Figure 8. Unfortunately, we were unable to analyze it using various fitting procedures. It is, however, clearly quite different from that of the corresponding crown.

B. Enantiomers of the Crown Isomer. *1. Solid-State Properties of the Neat Crown Enantiomers.* Because of the fast pseudorotation of the saddle isomer in solution it is not possible to separate it into its optical isomers. The crown isomer on the other hand is rigid and can be resolved into its enantiomers

with good optical purity as described in the Experimental Section. In the present section we describe the solid-state properties of these enantiomers and compare them with those of the crown racemate.

On the right-hand side of Figure 6 are shown DSC thermograms of the neat enantiomers, *A* and *B* (traces b and c, respectively). Both traces are essentially identical, but they differ considerably from that for the racemate (trace a). The neat enantiomers exhibit a first endothermic transition at around 130.4−135.1 °C followed by an exothermic peak at about 147 °C (see Table 2). Under a polarizing microscope, formation of liquid which immediately solidifies is observed in this temperature range. Eventually a second endothermic transition is observed at 202 °C which corresponds to melting of the crown racemate. The overall behavior is similar to that of the neat saddle (trace b on the left) and can be explained in a similar manner. In the present case the first endothermic peak corresponds to melting of the neat enantiomer; in the melt it undergoes rapid racemization and immediately crystallizes (exothermally) as the crown racemate, which melts on further heating at the melting point of the latter. The difference between the melting temperatures of the neat enantiomers and the racemate reflects their different structures (and stabilities) in their respective solid states.

The ^{13}C MAS spectra of the neat enantiomers are shown in the bottom two traces of Figure 7. The two spectra are essentially identical, and their multiplets can readily be identified as indicated in the figure. The peaks are quite sharp, and the spectra are reasonably well resolved, indicating that the samples are (poly) crystalline. The spectra are, however, quite different from that of the racemate (trace a). This is most clearly seen in the signal of carbon 1, which shows two triplets as compared with just one triplet for the corresponding carbon in the racemate. Careful examination of the enantiomers' spectra shows a similar doubling (of the triplets) in the other bands as well. These results indicate that for the neat enantiomers there are two symmetry unrelated molecules per asymmetric unit and that, as in the racemate, the molecules are distorted from C_3 symmetry.

The difference between the crystal structure of the enantiomers and that of the racemate is also manifested by their powder X-ray diffraction profiles. These diffraction patterns are shown in traces d and e of Figure 8. They are essentially identical and clearly correspond to polycrystalline samples. They differ considerably from that of the racemate (trace a); unfortunately, here too in the absence of large single crystals we were unable to determine the crystal structure of the enantiomers.

2. Solution NMR Spectra. The ^1H and ^{13}C spectra of the crown enantiomers in normal (achiral) solvents are identical to those of the racemate, as described above. Their spectra in chiral liquid crystals show clear discrimination due to their selective ordering in such phases. This effect was studied in detail for a number of deuterated and carbon-13-enriched isotopomers of **1** dissolved in poly-γ-benzyl-L-glutamate-based lyotropic solvents. The results of this study are published elsewhere.[13] As indicated above, spectra recorded in such a solvent could be used to check the enantiomeric purity of the separated samples. Except for a few samples, these results showed perfect separation with no or very little enantiomeric contamination.

We have not performed kinetic studies on the rate of racemization in solution. For the case of the chiral CTV-d_9 the mechanism of this process was shown to proceed via the saddle form,[11,30] and it is most likely the same for **1**.

3. Optical Rotation. The optical rotation of the separated enantiomers was measured in chloroform solution at room temperature (20 °C). Preliminary measurements were performed with solutions in the concentration range 5−10 mg/mL, yielding optical rotations of less than 0.1°. The final measurements were therefore performed on 10-fold more concentrated solutions, yielding rotations of several tenths of a degree. Measurements were taken for the Na line (589 nm) and several of the Hg lines. The results for the specific rotations are summarized in Table 3. For all wavelengths the *A* enantiomer was found to be levorotatory (−), while *B* is dextrorotatory (+). The magnitudes of the specific rotations, $[\alpha]_\lambda^{20}$'s, are quite small compared to the chiral hexasubstituted cyclotriveratrylenes studied by Canceill et al.[19] As for the latter, the specific rotations are wavelength dependent, increasing gradually with decreasing λ.

TABLE 3: Specific Optical Rotation [deg/(g/mL)·dm] for Solutions of the *A* and *B* Enantiomers in $CHCl_3$ Solutions[a]

	λ (nm)				
	589	578	546	436	365
$[\alpha]_\lambda^{20}(A)$[b]	−6.9	−7.6	−8.2	−11.2	−16.1
$[\alpha]_\lambda^{20}(B)$[c]	+7.1	+7.4	+8.2	+10.8	
$\lvert[\alpha]_\lambda^{20}(\mathrm{Ave})$[d]	7.0	7.5	8.2	11.0	16.1

[a] The estimated accuracy is ±3% except for the result of $\lambda = 365$ nm where it is ±6%. [b] Data derived from a solution containing 62.1 mg of *A* in 1.17 mL of solvent. The results are corrected for 4% impurity (saddle isomer) present in this particular sample. [c] Data derived from a solution containing 80.7 mg of *B* in 1.18 mL of solvent. [d] Average values of the magnitudes of the specific optical rotation.

4. UV and UVCD Spectra. The UV and UV−circular dichroism (UVCD) spectra of enantiomers *A* and *B* were measured in ethanol solutions (0.2−0.3 mM) at room temperature (20 °C). Examples of spectra are shown in Figure 9. In general, these results are similar to those obtained for other chiral cyclotriveratrylenes. The shoulder at 230 nm and the peak at 280 nm are related[15,16] to the $A_{1g} \rightarrow B_{1u}$ and $A_{1g} \rightarrow B_{2u}$ transitions of (unsubstituted) benzene with transition moments parallel, respectively, to the long and short axes of the benzene ring. Both transitions exhibit circular dichroism as seen in the upper part of the figure. The CD spectra of the two enantiomers are related by almost perfect reflection symmetry, confirming the satisfactory chiral separation. The CD of the B_{1u} signal consists of a single band, while that of B_{2u} exhibits a clear, although asymmetric, couplet with a negative chirality for the *A* enantiomer (negative Cotton effect at long λ's and positive at short λ's). An opposite chirality applies to *B*.

The couplet structure (exciton splitting) in the CD spectrum results from an interaction between transition moments in neighboring chromophores.[31] If their directions in the frames of the chromophores are known, the effect may be used to determine the absolute configuration of the enantiomers. This so-called exciton chirality method was employed by Collet and Gottarelli[15−23] to study hexasubstituted cyclotriveratrylenes with C_3 symmetry ($R_3 = H$, $R_1 \neq R_2$). In these compounds the effect results from through-space interactions between transition moments in the aromatic subunits of the TBCN core. Their optical activity arises from the substituent-induced rotation (θ in Figure 2) of the B_{2u} transition moment from the short axis of the benzene ring. In fact, these authors used the known configuration of their cyclotriveratrylenes to determine the substituent effect (spectroscopic moment) on the orientation of the transition moment,

To apply the (exciton chirality) method to the enantiomers of compound **1** we recall that[15,19] for the cyclotriveratrylenes $\theta > 0$ (and $|\theta| < 45°$) results in negative optical chirality (as observed for *A*) while $\theta < 0$ results in positive chirality (as observed for *B*). We are, however, unable to guess the sign of

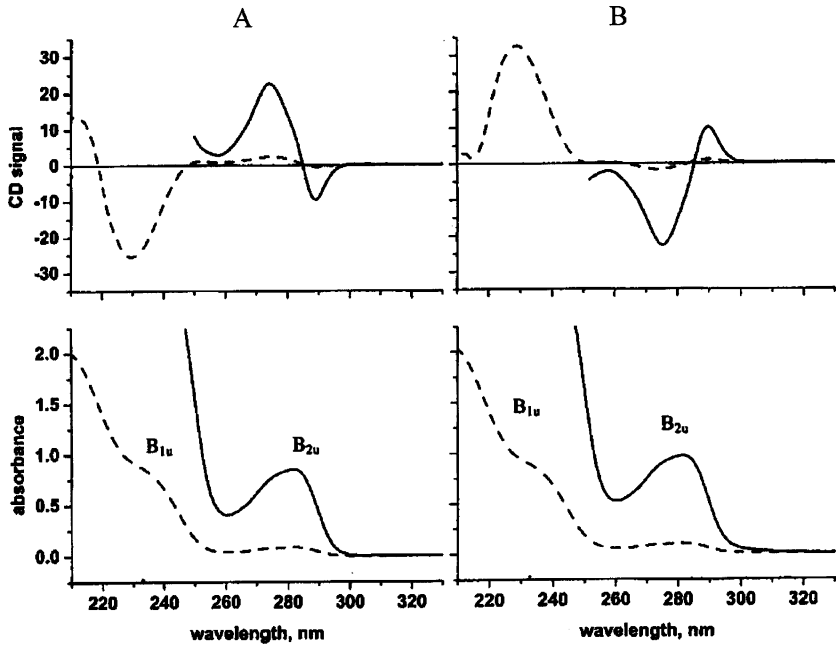

Figure 9. Room-temperature UV (bottom) and UVCD (top) spectra of solutions of enantiomers *A* (left) and *B* (right) (0.23 and 0.25 mM, respectively) in ethanol. Full and dashed lines correspond to cells with optical lengths of 10 and 1 mm, respectively.

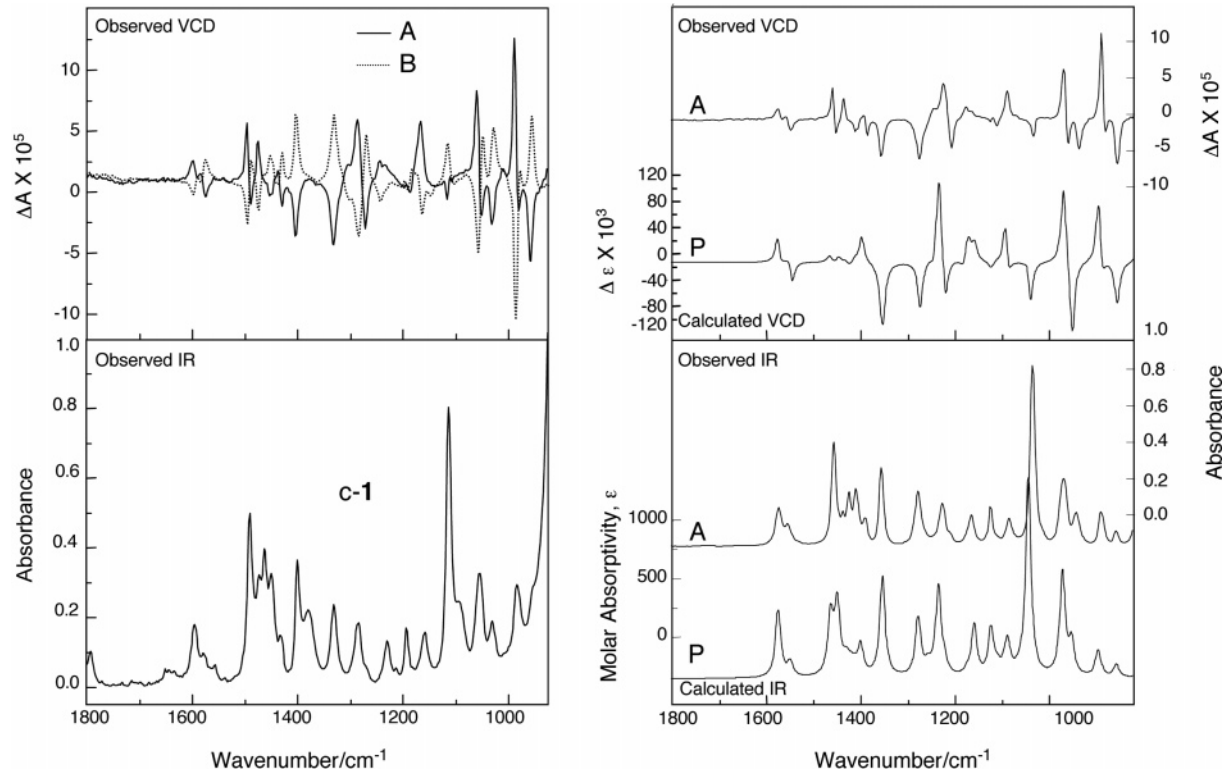

Figure 10. (Bottom left) Experimental (solvent subtracted) IR spectrum of a racemic mixture of **1** (4 mg in 0.12 mL of $CDCl_3$). (Top left) Experimental VCD spectra of the *A* (solid line) and *B* (dotted line) enantiomers (same concentration as for the IR spectrum of the racemate). The traces on the right compare the observed IR (bottom) and VCD (top) spectra of enantiomer *A* with those calculated for the *P* configuration.

θ from the substitution pattern of the methoxy groups in c-**1**. From the spectroscopic vector addition rule[32] it follows that, to first order, 1,2,3-substitution of benzene with identical substituents should have no effect on the transition moment. Its chirality should therefore be of second order and the magnitude of θ small. Being unable to estimate θ, we reverse the procedure and determine its sign from the configurations of *A* and *B* as derived (see next section) by VCD. There we show that *A* and *B* correspond, respectively, to configurations *P* and *M*. Hence, $\theta < 0$ for the former and $\theta > 0$ for the latter.

5. IR and VCD. For molecules of moderate complexity VCD provides a most powerful tool for determining the absolute configuration of optically active isomers.[24,25] The recent developments in instrumentation, on the one hand, and in the software for quantum mechanical calculation of VCD spectra, on the other, provide unambiguous results with essentially zero uncertainty in the identification of the enantiomers. An impressive example of this application is the recent determination of the absolute configuration of cryptophane-A, a molecule having about twice the size of compound **1** and like the latter exhibiting

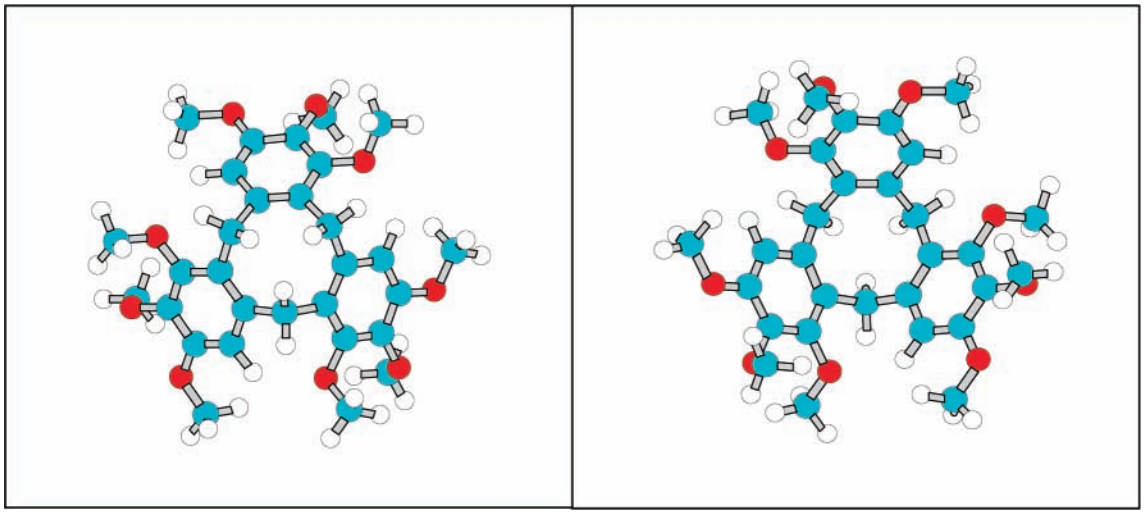

Figure 11. Optimized geometry of the *P* enantiomer, viewed from above (left) and below (right) the TBCN core, along the C_3 axis. The methoxy groups are, respectively (see Figure 1b), in the plane of the benzene rings (R_1), below the plane toward the C_3 axis (R_2), and above this plane (R_3).

structural chirality.[33] The power of this method is also demonstrated below for the crown enantiomers of **1**. In fact, even the small perturbation in the spectra brought about by isotopic substitution could be accurately reproduced by the calculations (not shown below), lending even stronger support to the enantiomeric assignment.

Examples of IR and VCD spectra of enantiomers *A* and *B* of the isotopically normal compound **1** at room temperature are shown on the left side of Figure 10. The IR spectrum of only the racemate is displayed; those of the neat enantiomers are essentially identical to the latter. On the other hand, the VCD spectra of the enantiomers display almost perfect mirror symmetry, confirming the optical purity of the samples. On the right-hand side of Figure 10 the experimental IR (bottom) and VCD (top) spectra of the *A* enantiomer are compared with calculated traces for the *P* configuration (see Figure 2). To eliminate possible small baseline artifacts the calculated spectrum was actually compared with one-half of the difference of the experimental VCD spectra, 1/2[VCD(*A*) − VCD(*B*)]. The near-perfect agreement between the observed and calculated spectra establishes the configuration of enantiomer *A* as *P* and of *B* as *M*.

The theoretical VCD was calculated for a single conformation obtained by energy minimization, using DFT, over a broad distribution of the orientation of the methoxy groups around the TBCN core. The similarity of the experimental and calculated spectra thus suggests that a single conformation dominates the conformational distribution. This is shown for the *P* enantiomer in Figure 11. The initial structure with all methoxy groups in the planes of the benzene rings optimized to a structure with one (R_1) methoxy group remaining in the plane, one below the plane toward the C_3 axis (R_2), and one (in the ortho position) above the plane (R_3), for each benzene ring, thus maintaining the C_3 symmetry. Examination of the calculated structure indicates that rotation of the out of plane methoxy groups to the opposite sides of the benzene plane would introduce unfavorable steric overlap with the in-plane methoxy group on the adjacent ring.

Summary and Conclusions

The occurrence of the saddle form in substituted cyclotriveratrylenes is apparently more universal than previously thought and not limited to the sterically hindered and ring-modified TBCN core. The failure to detect the saddle isomers in peripherally substituted and weakly hindered cyclotriveratrylenes stems from the synthetic procedure. Acidic trimerization of the appropriate benzyl alcohol at moderate temperatures, as usually employed in the synthesis, favors the crown isomer. Any saddle isomer formed under these conditions would be washed out during the purification step. Moreover, it will usually not be reformed on standing because its formation rate and equilibrium concentration at room temperature are very low. The saddle isomer can however be produced quantitatively by a heating/quenching cycle in which a solution of the compound is heated to a high temperature, where the saddle isomer is favored, followed by quenching and separation at room temperature. In the present work we applied this method to nonamethoxy-TBCN, which was previously believed to exist only as the crown isomer. We investigated the crown/saddle isomerization in solution and studied the solid-state properties of both isomers in the solid state by ^{13}C NMR and X-ray techniques. Unusual DSC thermograms were observed, reflecting the different melting transitions of the two isomers and their different equilibrium concentration in the melt.

The crown and saddle isomers of nonamethoxy-TBCN have, respectively, C_3 and C_1 symmetries and are therefore chiral, but the synthesis results in racemic mixtures. The fast pseudorotation of the saddle isomer precludes its separation into enantiomers, but the rigid crown form lends itself to such enantioseparation by HPLC using suitable chiral columns. We investigated the solid-state properties of the crown enantiomers and compared them with the racemate. The neat enantiomers are stable in the solid state, but they melt at a considerably lower temperature than the racemate, and in the melt they rapidly racemize, most likely via the saddle form. Their crystal structures differ significantly from that of the racemate; the latter contains a pair of enantiomeric molecules per unit cell, related to each other by inversion symmetry, while the neat enantiomers contain two, symmetry unrelated, molecules per asymmetric unit. The different melting transition of the neat enantiomers and the racemate and the fast racemization in the melt results in characteristic DSC thermograms similar to those observed for the neat saddle.

In a separate publication[13] we studied the NMR spectra of the racemate and neat enantiomers in chiral liquid crystalline solvents. Here we extended these studies to the optical properties of such solutions, including UV circular dichroism (UVCD) and IR circular dichroism (VCD). The UVCD spectra were similar

to those obtained for chiral peripherally substituted cyclotriveratrylenes,[15−23] exhibiting clear exciton splitting. The effects were, however, difficult to interpret in terms of the absolute configuration of the enantiomers. This difficulty stems from the uncertainty in evaluating the effect of multiple spectroscopic moments on the final transition moment. Such an evaluation requires quantum mechanical computation of electronically excited states, which are very demanding. On the other hand, the absolute configuration of the enantiomers could readily be derived from analysis of the VCD spectra. In particular, we found that the first and second enantiomers to elute from the separation column correspond, respectively, to the *P* and *M* configurations of Figure 2. Such an analysis requires quantum mechanical calculations of vibrational spectra in the ground electronic state only, which can readily be performed at a high level of accuracy on molecules of the size discussed here.

An interesting extension of this study could be toward long-chain substituted cyclotriveratrylene. Such compounds are known to exhibit columnar mesophases with different structures. The peripherally substituted derivatives (with C_{3v} symmetry) are, however, so far only known in the crown form.[6,7] It would be interesting to determine whether the saddle form of such compounds also exists (as we believe), whether they are mesogenic, and if so determine their mesogenic properties. Long-chain nonaalkanoyloxy cyclotriveratrylenes (C_3 symmetry) are known to be mesogenic in both the saddle and crown forms.[10] So far, however, they were only studied as racemates. The successful separation of the nonamethoxy cyclotriveratrylene derivative into its enantiomers raises the hope that the same procedure may also be used for the higher mesogenic homologues. This will open the way to prepare and study chiral columnar mesophases based on chiral cores (rather than chiral side chains).

Acknowledgment. We thank M. Sheves and G. Gottarelli for helpful discussions concerning UVCD; A. Tishbee, M. Fridkin, and A. Kapitkovsky for their help and suggestions concerning the HPLC separation, R. Fliash for help in measuring optical rotation, and M. Lahav and L. Leiserowitz for many discussions on structural chirality. This research was made possible in part by the historic generosity of the Harold Perlman Family.

References and Notes

(1) Lindsey, A. S. *Chem. Ind. (London)* **1963**, 823−824. Lindsey, A. S. *J. Chem. Soc.* **1965**, 1685−1692.

(2) Collet, A. *Tetrahedron* **1987**, *43*, 5725−5759.

(3) Garcia, C.; Andraud, C.; Collet, A. *Supramol. Chem.* **1992**, *1*, 31−45.

(4) Collet, A. *Comp. Supramol. Chem.* **1996**, *6*, 281−303.

(5) Andraud, C.; Garcia, C.; Collet, A. In *Circular Dichroism: Principles and Applications*, 2nd ed.; Berova, N., Nakanishi, K., Wooky, R. W., Eds.; Wiley-VCH: New York, 2000; Chapter 13.

(6) Zimmermann, H.; Poupko, R.; Luz, Z.; Billard, J. *Z. Naturforsch.* **1985**, *40a*, 149−160.

(7) Malthete, J.; Collet, A. *Nouv. J. Chim.* **1985**, *9*, 151−153.

(8) Canceill, J.; Lacombe. L.; Collet, A. *C. R. Acad. Sci. Ser. 2* **1984**, *298*, 39−42.

(9) Collet, A. *Comp. Supramol. Chem.* **1996**, *2*, 325−365.

(10) Zimmermann, H.; Bader, V.; Poupko, R.; Wachtel, E. J.; Luz, Z. *J. Am. Chem. Soc.* **2002**, *124*, 15286−15301.

(11) Zimmermann, H.; Tolstoy, P.; Limbach, H.-H.; Poupko, R.; Luz, Z. *J. Phys. Chem. B* 2**004**, *108*, 18772−18778.

(12) Lesot, P.; Merlet, D.; Sarfati, M.; Courtieu, J.; Zimmermann, H.; Luz, Z. *J. Am. Chem. Soc.* **2002**, *124*, 10071−10082.

(13) Lafon, O.; Lesot, P.; Zimmermann, H.; Poupko, R.; Luz, Z. *J. Phys Chem. B*, in press.

(14) Malthete, J.; Collet, A. *J. Am. Chem. Soc.* **1987**, *109*, 7544−7545.

(15) Collet, A.; Gottarelli, G. *J. Am. Chem. Soc.* **1981**, *103*, 204−205.

(16) Collet, A.; Gottarelli, G. *J. Am. Chem. Soc.* **1981**, *103*, 5012−5913.

(17) Collet, A.; Gottarelli, G. *J. Am. Chem. Soc.* **1982**, *104*, 7383−7384.

(18) Canceill, J.; Collet, A.; Gottarelli, G. *J. Am. Chem. Soc.* **1984**, *106*, 5997−6003.

(19) Canceill, J.; Collet, A.; Gabard, J.; Gottarelli, G.; Spada, G. P. *J. Am. Chem. Soc.* **1985**, *107*, 1299−1308.

(20) Canceill, J.; Collet, A.; Gottarelli, G.; Palmieri, P. *J. Am. Chem. Soc.* **1987**, *109*, 6454−6464.

(21) Collet, A.; Gottarelli, G. *Croat. Chem. Acta* **1989**, *62*, 279−292.

(22) Collet, A.; Gabard, J.; Jacques, J.; Cesario, M.; Guilhem, J.; Pascard, C. *J. Chem. Soc., Perkin Trans.* **1981**, *1*, 1630−1638.

(23) Tambute, A.; Canceill, J.; Collet, A. *Bull. Chem. Soc. Jpn.* **1989**, *62*, 1390−1392.

(24) Freedman, T. B.; Cao, X.; Dukor, D. K.; Nafie, L. A. *Chirality* **2003**, *15*, 743−758.

(25) Paterlini, M. G.; Freedman, T. B.; Nafie, L. A.; Tor, Y.; Shanzer, A. *Biopolymers* **1992**, *32*, 765−782.

(26) Bosch, J.; Canals, J.; Granados, R. *An. Quim.* **1976**, *72*, 709−712.

(27) Salmon, M.; Cabrera, A.; Zayala. N.; Espinoza-Perez, G.; Gardenas, J.; Gavino, R.; Cruz, R. *J. Chem. Cryst.* **1995**, *25*, 759−763. In this paper the number of molecules per unit cell is erroneously given as $Z = 4$ instead of 2.

(28) Krieger, C. (MPI for Medical Research, Heidelber, Germany) Personal communication, 1998. These measurements were done on a colorless prismatic crystal with dimensions 0.15 × 0.20 × 0.30 mm using an Enraf Nonius CAD4 circle diffractometer with a graphite monochromator (Mo Kα, $\lambda = 0.07107$ nm) and applying the $\omega - 2\theta$ scanning technique. The structure was solved and refined as described earlier.[29]

(29) Müller, K.; Zimmermann, H.; Krieger, C.; Poupko, R.; Luz, Z. *J. Am. Chem. Soc.* **1996**, *118*, 8006−8014.

(30) Collet, A.; Gabard, J. *J. Org. Chem.* **1980**, *45*, 5400−5401.

(31) Harada, N.; Nakanishi, K. *Circular Dichroic Spectroscopy−Exciton Coupling in Organic Stereochemistry*; University Science Books: Mill Valley, CA, 1983.

(32) Platt, J. R. *J. Chem Phys.* **1951**, *19*, 263−271.

(33) Brotin, T.; Cavagnat, D.; Dutasta, J.−P.; Buffeteau, T. *J. Am. Chem. Soc.* **2006**, *128*, 5533−5540.